

pubs.acs.org/JPCB Article

Significant Enhancement of Two-Photon Excited Fluorescence in Water-Soluble Triphenylamine-Based All-Organic Compounds

Yu Gong,* Xiangdong Bi,* Nikki Chen,* Marcello Forconi,* Narayanan Kuthirummal, Alem Teklu, Bo Gao, Jacob Koenemann, Nico Harris, Christian Brennan, Marisa Thomas, Taylor Barnes, and Ming Hu*



Cite This: J. Phys. Chem. B 2022, 126, 5513-5522



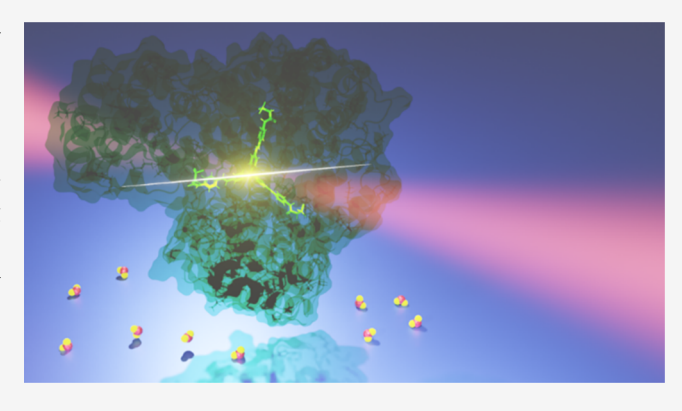
ACCESS

III Metrics & More



Supporting Information

ABSTRACT: Understanding water-soluble and environmentally friendly two-photon absorption (TPA) molecules benefits the design of superior organic complexes for biomedical, illumination, and display applications. In this work, we designed two triphenylamine-based all-organic compounds and explored the mechanism of enhanced TP fluorescence in water solutions for potential applications. Experimentally, we showed that adding protein into our TPA molecule solution can drastically boost the TP fluorescence. Numerical simulations reveal that the TPA molecules prefer to dock inside the protein complex. We hypothesize that the interaction between our triphenylamine-based all-organic compounds and water molecules lead to non-radiative decay processes, which prevent strong TP fluorescence in the water solution. Therefore, the protection by, for example,



protein molecules from such interactions can be a universal strategy for superior functioning of organic TPA molecules. Further experiments and numerical simulations support our hypothesis. The present study may facilitate the design of superior water-soluble and environmentally friendly superior organic complexes.

I. INTRODUCTION

The fast development of biomedical, illumination, and display technologies requires more efficient and environmentally friendly materials that emit light with different wavelengths. Although traditional inorganic materials have been well developed to produce light with a broad spectral range, most of them are environmentally hazardous. Organic fluorescent materials show great potential as a low-cost and environmentally friendly alternative. 1 Organic fluorescent materials have already been used in fluorescent labeling for bioimaging,²⁻⁶ chemosensors,⁷⁻¹¹ and artificial lighting.¹² There is a strong demand for new two-photon absorption (TPA) materials for a wide range of applications, such as two-photon microscopy, ^{13–17} microfabrication, ^{18,19} three-dimensional data-storage, ^{20,21} up-converted lasing, ^{22,23} and photodynamic therapy. ^{24–26} TPA is a nonlinear effect, in which the material usually absorbs low-energy and long-wavelength photons in the near-infrared (NIR) range with a better penetration depth for human tissue and cause much less damage to the TPA molecules compared to the linear absorption effect. These advantages benefit microscopy, photodynamic therapy, and upconverted lasing applications. Furthermore, the light absorption rate for TPA is proportional to the square of light intensity, and thus the TPA works only at the very center

region of a focused laser beam, which enables the microfabrication and three-dimensional data storage with an even higher operation precision compared to lithography/polymerization using linear absorption materials. 27,28 To facilitate these applications, high TPA efficiency is one of the priorities for TPA molecules. However, TPA efficiency can be dominated by various factors. For example, the lifetime of an intramolecular charge separation state may have a strong impact on the TPA efficiency.²⁹ In addition, charge transport efficiency can be also an important factor that affects TPA efficiency. 30,31 Cooperative enhancement is effected through electronic and vibronic coupling³² and appropriate energy gaps.³³ Within various TPA molecules, organic multi-branched chromophore structures have attracted a lot of attention due to their excellent potentials. First, because of the electronic/vibronic coupling between different molecular branches, the TPA efficiency gets cooperatively enhanced.³⁴ Second, as the TPA efficiency

Received: May 20, 2022 Revised: June 30, 2022 Published: July 13, 2022





Scheme 1. Synthesis of Taurine-Functionalized Water-Soluble Two-Photon Chromophores

increases, the optical transparency decreases, while multibranched structures can be the solution for such nonlinearitytransparency trade-off.³⁵ Third, the optical excitation on the branches could induce efficient fluorescence resonance energy transfer to the core, which gives a significant increase in the fluorescence emission from the core.³⁶ In addition, multibranched structures can reduce the aggregating and selfquenching effect, which benefits the strong TP fluorescence.³⁷ Although the high efficiency of TPA is always a prerequisite for TPA applications and organic systems with multi-branched structures and various types of central cores that have been studied, 38-42 it does not guarantee the superior performance of TPA molecules in the abovementioned applications. As a more fundamental perspective, the implementation of TPA molecules for artificial lighting, microscopy, or up-converted lasing applications is crucially dependent on how well they can dissipate the absorbed energy in the form of light emission instead of through non-radiative decay processes. Therefore, understanding and designing organic TPA molecules with a higher fluorescence efficiency become important goals.^{43,44} In addition, the mass production of TPA molecules requires the organic molecule and its solvent to be biocompatible, environmentally friendly, and cost-efficient, which favors the TP fluorescent molecules to be water-soluble. While it is challenging, in principle, these requirements could be realized through manipulation of molecular configurations. 45,46 It is non-trivial to tune the way energy is released for organic TPA molecules while maintaining its environmental friendliness and biocompatibility. Exploring all organic TPA molecules with superior fluorescence emission not only can facilitate applications of organic TPA materials but also provides a direction for the optimization of other TPA materials.

In this work, we designed triphenylamine-based all-organic compounds and explored the mechanism of enhanced TP fluorescence for potential applications in organic devices. These molecules are strongly florescent due to enhanced chromophore density and extended conjugation by multibranched structures, the nitrogen lone pair that participates in conjugation, and the terminal carbonyl group that pulls electrons to enhance electron flow in the conjugation system. We made the triphenylamine-based all-organic compound become water-soluble, and to enhance the fluorescence, we mixed proteins with our triphenylamine-based all-organic compounds in water solution. Surprisingly, a significant enhancement of fluorescence (as large as 40-fold) was observed upon adding proteins to the solution. The centrifuge

experiment indicated the formation of strong and stable assemblies of protein complexes with our designed TPA molecules. Simulations show that the TPA molecules are more likely to dock inside the protein, which agrees with our centrifuge experiments. Based on our simulation results, we hypothesize that the hydrogen bond between the triphenylamine-based all-organic compounds and water creates nonradiative decay processes between the TPA excited states and the ground state so that the fluorescence is quenched. However, docking of our TPA molecule inside proteins prevents the formation of a hydrogen bond with water and resulted in the strong enhancement of TP fluorescence. Our experiments and numerical simulations turned out to be consistent with our hypothesis. Our findings may serve as a prototype for designing water-soluble and environmentally friendly superior organic complexes for biomedical, illumination, and display applications.

II. METHODS

II.A. Synthesis and Characterization of TPA Compounds 4 and 5. Chemicals including 4-vinylbenzoic acid, diethylamine, O-(benzotriazole-1-yl)-N,N,N',N'-tetramethyluronium hexafluorophosphate (HBTU), 1-hydroxybenzotriazole (HOBt), N,N-diisopropylethylamine (DIEA), acetic anhydride, triethylamine, tris(4-bromophenyl)amine, palladium acetate, tris(o-tolyl)phosphine, 2-aminoethanesulfonic (taurine), 1,5-diamiopentane, egg albumin (ALB), and solvents such as dimethylformamide (DMF), dimethyl sulfoxide (DMSO), tetrahydrofuran (THF), and protein concentrators PES were obtained from Fisher Scientific. Gelatin was purchased from FLINN Scientific. Arginine, spermine, and spermidine were ordered from Sigma Aldrich. Fetal bovine serum (FBS) was purchased from Thermo Fisher Scientific. Polyamidoamine dendrimer generations 0-5 (PAMAM dendrimers G0-G5) with amine terminal groups were ordered from Dendritech Inc. (Midland, MI, USA). Bovine albumin was ordered from MP Biomedicals, LLC. VEGF antibody, CD3e antibody, and fibronectin antibody were provided by Dr. Hua Wei, Medical University of South Carolina (MUSC).

Nuclear magnetic resonance (NMR): 1 H and 13 C NMR spectra of all compounds were recorded using a Varian 400 MHz spectrometer (Santa Clara, CA, USA). Matrix-assisted laser desorption/ionization time-of-flight (MALDI-TOF): MALDI mass spectrometry data was acquired on a Voyager DE-STR in positive ion reflector TOF mode. Samples were mixed on target with 0.75 μ L of 10 mg/mL 2,5-

dihydroxybenzoic acid and air-dried. Instrument settings were as follows: +20 kV acceleration voltage; 75% grid voltage; 150 ns delayed extraction; 100 shots per spectrum (typically 2–3 accumulated); 337 nm nitrogen gas laser; 20 Hz; 200–2000 m/z.

I.A.a. N,N-Diethyl-4-vinylbenzamide (2). To a 25 mL round-bottom flask were added 4-vinylbezoic acid (1) (138 mg, 1 mmol), diethyl amine (148 mg, 2 mmol), HBTU (758 mg, 4 mmol), and HOBt (306 mg, 2 mmol) (Scheme 1). The mixture was dissolved in DMSO (5 mL). The color of the solution turned yellow immediately. DIEA (516 mg, 4 mmol) was added to the mixture. The reaction mixture was stirred at room temperature overnight. The reaction mixture was poured into water and extracted with ethyl acetate (20 mL \times 3). The organic solution was isolated, dried over magnesium sulfate, and evaporated. The residue was purified on a silica gel column and eluted with hexanes:ethyl acetate 2:1. Pure product 2 was obtained as an oil (0.819 g, yield 100%). ¹H NMR (CDCl₃, 400 MHz) δ 7.37 (d, 2 H), 7.27 (d, 2H), 6.65 (dd, 1H), 5.72 (d, 1H), 5.23 (d, 1H), 3.47 (br, 1H), 3.20 (br, 1H), 1.16 (br, 1H), 1.05 (br, 1H). ¹³C NMR (CDCl₃, 100 MHz) 171.00, 138.28, 136.49, 136.01, 114.84, 43.23, 39.23, 14.17, 12.85.

I.A.b. (E,E,E)-Tris(4-(2-(4-N,N-diethylcarbamoylphenyl)ethenyl)phenyl)amine (3). To a 25 mL round-bottom flask were added tris(4-bromophenyl)amine (210 mg, 0.437 mmol), N,N-diethyl-4-vinylbenzamide (2) (266 mg, 1.301 mmol), palladium acetate (29.3 mg, 0.131 mmol), and tri(o-tolyl)phosphine (79.8 mg, 0.262 mmol). The mixture was dissolved in dry DMF (3 mL). Triethylamine (674.5 mg, 9.369 mmol) was added to the solution. Nitrogen was bubbled into the solution for 1 min to replace the oxygen in the flask. Fluorescence was observed after the reaction was heated to 100 $^{\circ}$ C. The mixture was continued to stir under 100 $^{\circ}$ C for 3 days. The mixture was poured into water and was extracted with methylene chloride (20 mL \times 3). The organic solution was collected and dried over anhydrous magnesium sulfate. The solvent was evaporated. Purification of the crude product by a silica gel column (methylene chloride:methanol 10:1) gave the pure product (0.283 g) in yellow powder (yield: 76.4%). 1 H NMR (CDCl₃, 400 MHz) δ 7.52 (d, 6H), 7.43 (6H), 7.37 (6H), 7.12 (d, 6H), 7.09 (d, 3H), 7.02 (d,3H), 3.53 (br 6H), 3.31 (br 6H), 1.21 (br 18H). ¹³C NMR (CDCl₃, 100 MHz) 171.09, 146.82, 138.40, 135.97, 131.98, 129.02, 127.61, 126.88, 126.61, 126.23, 124.29, 43.26, 39.25, 14.20, 12.96.

I.A.c. (E,E,E)-Tris(4-(2-(4-carboxylphenyl)ethenyl)phenyl)amine (4). Compound 3 (47 mg, 0.0554 mmol) was dissolved in THF (2 mL). To this mixture was added a Claisen base solution, which was made by dissolving potassium hydroxide (0.704 g, 0.0176 mol) in water (0.488 mL) and diluting with methanol (2 mL). The reaction mixture was heated to reflux at a 75 °C oil bath and maintained at that temperature overnight. The mixture was neutralized until it was slightly acidic. The solvent was evaporated. The solid residue was loaded on a silica gel column. The pure product was eluted with methylene chloride:methanol 10:1 as a yellow solid (25.1 mg, yield: 66.5%). ¹H NMR (CD₃OD, 400 MHz) δ 7.98 (d, 6 H), 7.61 (d, 6H), 7.52 (d, 6H), 7.28 (d, 3H), 7.13 (d, 3H), 7.07 (d, 6H). ¹³C NMR (CD₃OD, 100 MHz) 168.29, 147.01, 142.29, 132.10, 130.29, 129.80, 128.90, 127.65, 125.99, 125.82, 123.97. MS (MALDI-TOF) m/z calcd for $C_{45}H_{33}NO_6$, 683.2; found, 683.6.

I.A.d. Compound **5**. Compound **4** (16 mg, 0.0234 mmol), taurine (9.7 mg, 0.0776 mmol), HBTU (53.2 mg, 0.141 mmol), and HOBt (21.5 mg, 0.140 mmol) were dissolved in DMSO (1.5 mL). DIEA (36.2 mg, 0.0281 mmol) was added to the mixture. The color turned orange red immediately. Nitrogen gas was bubbled into the solution for 1 min to replace the air in the reaction flask. The reaction mixture was stirred at room temperature for 2 days. The color of the mixture turned yellow. TLC analysis indicated that all the starting material was reacted. The reaction mixture was loaded on a silica gel column, and the product was eluted by methylene chloride:methanol 2:1 as a yellow solid (21.8 mg, yield: 92.7%). ¹H NMR (CD₃OD, 400 MHz) δ 7.81 (d, 6 H), 7.63 (d, 6H), 7.54 (d, 6H), 7.27 (d, 3H), 7.13 (d, 3H), 7.10 (d, 6H), 3.81 (t, 6H), 3.09 (t, 6H). ¹³C NMR (CD₃OD, 100 MHz) 168.00, 147.00, 141.10, 132.41, 132.19, 129.81, 127.56, 127.26, 125.95, 123.96, 49.88, 35.74. MS (MALDI-TOF) m/zcalcd for C₅₁H₄₈N₄O₁₂S₃, 1004.2; found, 1004.8.

I.A.e. G5-Ac100. PAMAM dendrimer G5 (92.7 mg, 0.00349 mmol) was added to a 50 mL round-bottom flask and was dissolved in methanol (10 mL). Triethylamine (73.5 mg, 0.542 mmol) was added to dendrimer solution and was stirred for 5 min. A solution of acetic anhydride (42.7 mg, 0.419 mmol) in methanol (10 mL) was added dropwise. The resulting solution was allowed to stir at room temperature overnight. The mixture was transferred to a 100 mL stirred cell equipped with a 10,000 molecular weight cutoff (MWCO) membrane and was washed with phosphate buffered saline (PBS, 20 mL \times 3) and deionized water (20 mL \times 3). Lyophilization of the aqueous solution yielded the solid product (106 mg, yield: 97.1%). ¹H NMR integration indicated that all 110 amino terminal groups were acetylated. (1H and 13C NMR spectra of compounds 2-5 can be found in Figure S3a-h in the Supporting Information).

II.B. Optical Measurements. The TP fluorescence measurements were carried out by combining our femtosecond laser system (KMLabs Collegiate — Ti:sapphire Laser) and the Ocean Optics SD2000 spectrometer. Our femtosecond laser system delivers ultrashort laser pulses with an average power of approximately 650 mW at a repetition rate of 90 MHz. The pulse duration is about 50 fs. The bandwidth, estimated as the full width at half maximum (FWHM) of the spectrum profile, is 51 nm, and the spectrum is centered at 800 nm. The incident laser power was measured using a digital power meter prior to each measurement of the sample.

II.C. Sample Preparation for Fluorescence Emission Measurement. All protein stock solutions (albumin, gelatin, FBS, PAMAM dendrimers, and other amine compounds) were prepared at 1.3 mg/mL in PBS buffer. Compounds 4 and 5 were dissolved in DMSO at a concentration of 0.0141 M. Both concentrations of proteins and dyes are not optimized and can be verified depending on the solubility of the materials and specific application. In this research, samples of protein and dye solutions for fluorescence measurement were made by mixing a 5.1 μ L DMSO solution of compound 4 or 5 with a 100 μ L protein solution. The final concentration of dye was 6.8 \times 10⁻⁴ M.

II.D. Computational Methods. The molecular docking simulation was performed to help gain a better understanding of the interactions behind the dye—protein florescence. The ligands were created on ChemDraw 20.1.1 (PerkinElmer Informatics), and the SMILES (Simplified Molecular Input Line Entry Specification) formulas were converted into PDB

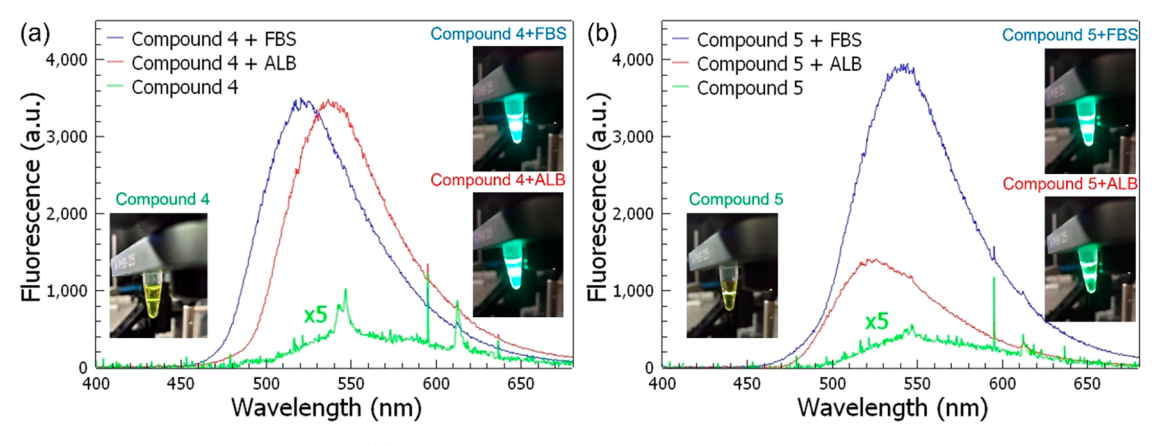


Figure 1. TP fluorescence spectra for compounds (a) 4 and (b) 5 in the PBS solution mixed with protein FBS and ALB under the excitation of 800 nm femtosecond laser. Insets of (a) and (b) are the images of TP fluorescence for the six samples with the same dye and protein concentrations.

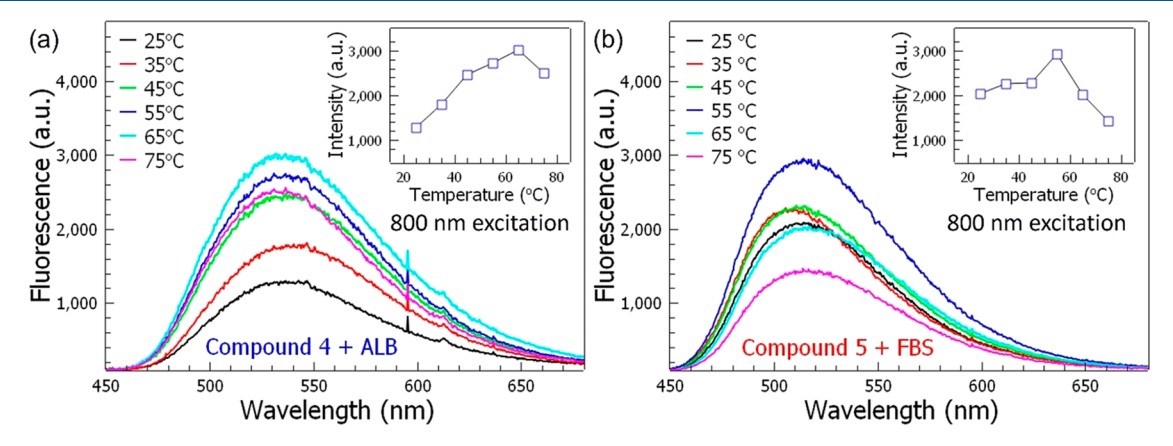


Figure 2. TP fluorescence spectra for (a) compound 4 and (b) compound 5 mixed with protein ALB and FBS under different temperatures. Insets of (a) and (b) are the plots of fluorescence peak intensities as a function of temperature. All the two-photon fluorescence spectra were measured at room temperature. The temperatures listed in the figure are the protein and TPA molecule mixture preparation temperatures.

(Protein Data Bank) files with optimized 3D structures using Avogadro. The bovine serum albumin (BSA) receptor was obtained from RCSB (Research Collaboratory for Structural Bioinformatics) PDB (PDB ID 4F5S). The PDB files of the ligands and proteins were converted to PDBQT files, and appropriate ligand—dye grid coordinates were found using AutoDock tools. The docking simulation was performed using AutoDock Vina, and the results were interpreted with the PyMOL Molecular Graphics System, Version 2.0 (Schrödinger, LLC).

III. RESULTS AND DISCUSSION

III.A. Experimental TP Fluorescence Spectra. The fluorescent photons obtained with the 800 nm excitation were collected by an optical lens and focused into a fiber coupled spectrometer. All the samples emitted photons with a much higher energy than the excitation photon (800 nm), revealing that the fluorescence is a nonlinear multiphoton absorption process. The TP fluorescence spectra for compound 4 (Figure 1a) in PBS solution mixed with protein FBS and ALB as well as compound 5 (Figure 1b) in PBS solution mixed with protein FBS and ALB were all measured under ambient conditions. Compounds 4 and 5 in PBS solution without protein displayed a very weak TP fluorescence with maxima at 550 nm (optical image and spectra intensity, green spectrum in Figure 1a,b). We measured TP fluorescence in pure water, in phosphate solution, in PBS

solution, and in HCl solution, and they all showed similar weak TP fluorescence (Figure S1 in the Supporting Information). However, when the proteins FBS (blue spectrum) or ALB (red spectrum) are mixed with compound 4 or 5 in PBS solutions, a significant enhancement of fluorescence was observed under femtosecond laser excitation. The maximum enhancement was as large as 40-fold: compound 5 + FBS versus compound 5 only in PBS solution. The enhancement to compound 4 when mixed with protein was also about 35-fold. In addition, we noticed that the fluorescence spectra of compound 4 or 5 mixed with protein in PBS are all blue shifted compared to those of compound 4 or 5 only in PBS solutions. The images in Figure 1a,b also show that the fluorescence colors of compound 4 or 5 with protein solutions are all green but those of compound 4 or 5 only solutions are yellow, indicating that the molecular interactions exist between compound 4 or 5 with protein FBS or ALB in PBS. Additionally, there is a relative shift between the fluorescence spectra of compound 4 or 5 with protein FBS or ALB, which will be discussed later.

To understand the fluorescence enhancement with the addition of protein in the TPA solution, we first prepared samples under various temperatures by mixing TPA molecules and protein in water and TP fluorescence was measured at room temperature. Figure 2 displays the TP fluorescence spectra for compound 4 (Figure 2a) and compound 5 (Figure 2b) mixed with protein ALB and FBS, respectively, under different temperatures. As shown in Figure 2, the TP

fluorescence spectra of compounds 4 and 5 are temperaturedependent. We plot the peak intensities of TP fluorescence spectra as a function of mixing temperature in the inset of Figure 2a,b for compounds 4 and 5, respectively. Apparently, the maximum fluorescence intensity first increases and then starts to decrease with increasing mixing temperature. The optimal fluorescence intensity appears around 60 °C for both molecules. This trend suggests that there is an interaction between TPA molecules and protein that is crucial to the TP fluorescence when they are mixed in the water solution. The process can be hypothesized as follows: when mixed at a comparatively low temperature, the majority of TPA molecules may not reach the best interaction position with proteins since temperatures highly affect the orientation of the protein complex. However, when the temperature is increased, most of the TPA molecules receive more kinetic energy so that they are able to find the optimal interaction position with protein. Also, proteins are likely to start unfolding upon increasing the temperature, increasing molecular interactions. If the temperature is further increased, the denaturation of the protein starts. Indeed, it is known that BSA starts to denature around 60 °C, 50 which is consistent with the observations reported in Figure 2.

III.B. Numerical Docking Simulation. To further understand the interaction between the dye and protein molecules, we employed numerical calculations to simulate the docking of dye molecules in proteins. Based on our experimental results, the solution containing the dye and fetal bovine serum (FBS) solvent showed a significant increase in the intensity of fluorescence compared to dye in PBS solution. FBS is often used as a growth supplement for cells and contains a high protein concentration and other components such as electrolytes, hormones, lipids, and carbohydrates. Since FBS solvent contains various components (proteins), the docking procedure cannot be used to analyze FBS and the dye directly. However, bovine serum albumin (BSA) is the major protein in FBS (2.5 mg/mL) and indeed we also see the fluorescence enhancement when dye is mixed with BSA only (Figure S2 in the Supporting Information). Therefore, the docking simulations were performed on compounds 4 and 5 with BSA as the receptor. Figure 3a,b displays the docking simulation results for compounds 4 and 5 with BSA, respectively. BSA is in cyan with the side chains histidine, lysine, and arginine residues in light orange. Compounds 4 and 5 are in purple, gray, and red colors. The best affinity binding states for the

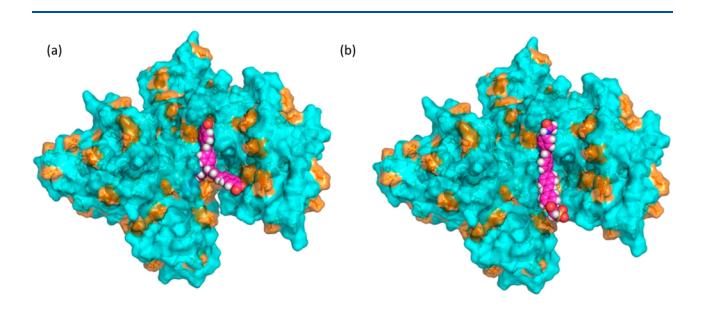


Figure 3. Docking simulation of dye molecules with BSA. (a) Compound 4 docking with BSA. (b) Compound 5 docking with BSA. The lysine, arginine, and histidine side chains are in light orange, while the protein is in cyan. The simulation figure shows the best affinity of protein–ligand binding. A total of nine binding states were performed, and their relative affinity is included in the Supporting Information (Tables S1–S3).

docking for compounds 4 and 5 with BSA are shown in Figure 3. Although the orientations of docking for compounds 4 and 5 are slightly different (Figure 3a,b), both compounds are largely enclosed by BSA and they are situated inside the BSA hydrophobic core. In previous research describing the interaction between dye and water molecules, researchers have demonstrated that the existence of water molecules strongly quenches the fluorescence through the nonradiative relaxation process.⁵¹ In our case, the solution without protein displayed a very weak fluorescence. After docking with protein molecules, the highly hydrophobic environment inside BSA where dye molecules dock seems to contribute to the enhancement of fluorescence from dye molecules. Therefore, we hypothesize that the interaction of BSA with the dye molecules would isolate the dye from interacting with water molecules, preventing the quenching of fluorescence.

III.C. TP Fluorescence and Numerical Simulation of **Docking with Dendrimers.** To further test our hypothesis, the TP fluorescence measurements were performed for dye compound 5 in solutions containing polyamidoamine (PAMAM) dendrimers. The PAMAM dendrimers are hyperbranched polymers with terminal amine groups. As the generation increases, the complexity and size of the dendrimer increase. We expect that the interaction between dye molecules and dendrimers with evolving complexity would create a similar hydrophobic docking environment, which enhances the fluorescence strength. Figure 4a shows the TP fluorescence spectra for dye compound 5 mixed with different dendrimers. As the complexity of the dendrimers increases, a significant enhancement of the TP fluorescence can be observed. Figure 4b shows the maximum fluorescence intensity as a function of amino functional group number (indicating the increasing complexity of the molecule) in the dendrimers. Guided by the red solid line in Figure 4b, although the fluorescence intensity increases, it is obvious that the enhancement starts to slow down when the dendrimer becomes increasingly complex. This indicates that the fluorescence cannot be infinitely enhanced but has a saturation level as the generations of the dendrimer increases. To obtain further insight, we employed simulations again to dock compound 5 with three different PAMAM dendrimer molecules, as shown in Figure 4c. Specifically, we docked compound 5 molecules with generation 1 (G1), generation 3 (G3), and generation 5 (G5) PAMAM dendrimers because of the increased complexity through generations. According to the simulation results, although dye compound 5 interacts with the G1 dendrimer, it is largely exposed to the solvent environment. The G3 dendrimer encloses nearly half of the volume of dye compound 5, while the G5 dendrimer almost completely encloses the dye molecule, similar to the docking with BSA. The simulation results indicate that G1 does not efficiently prevent compound 5 from interacting with the solvent environment. G3 only partially encloses compound 5, which still allows some level of dye interaction with the solvent environment. G5 entirely encloses compound 5, which best protects the dye from the solvent environment. As the generation increases, the dye molecules experience a stronger hydrophobic environment, which makes it less likely to interact with the solvent environment. Since the dye and dendrimers are all in the water solution, water molecules potentially provide most interactions in our experiments. Previous results reveal that interaction of the dye molecules with water decreases the intensity of the fluorescence significantly.⁵¹ Therefore, our

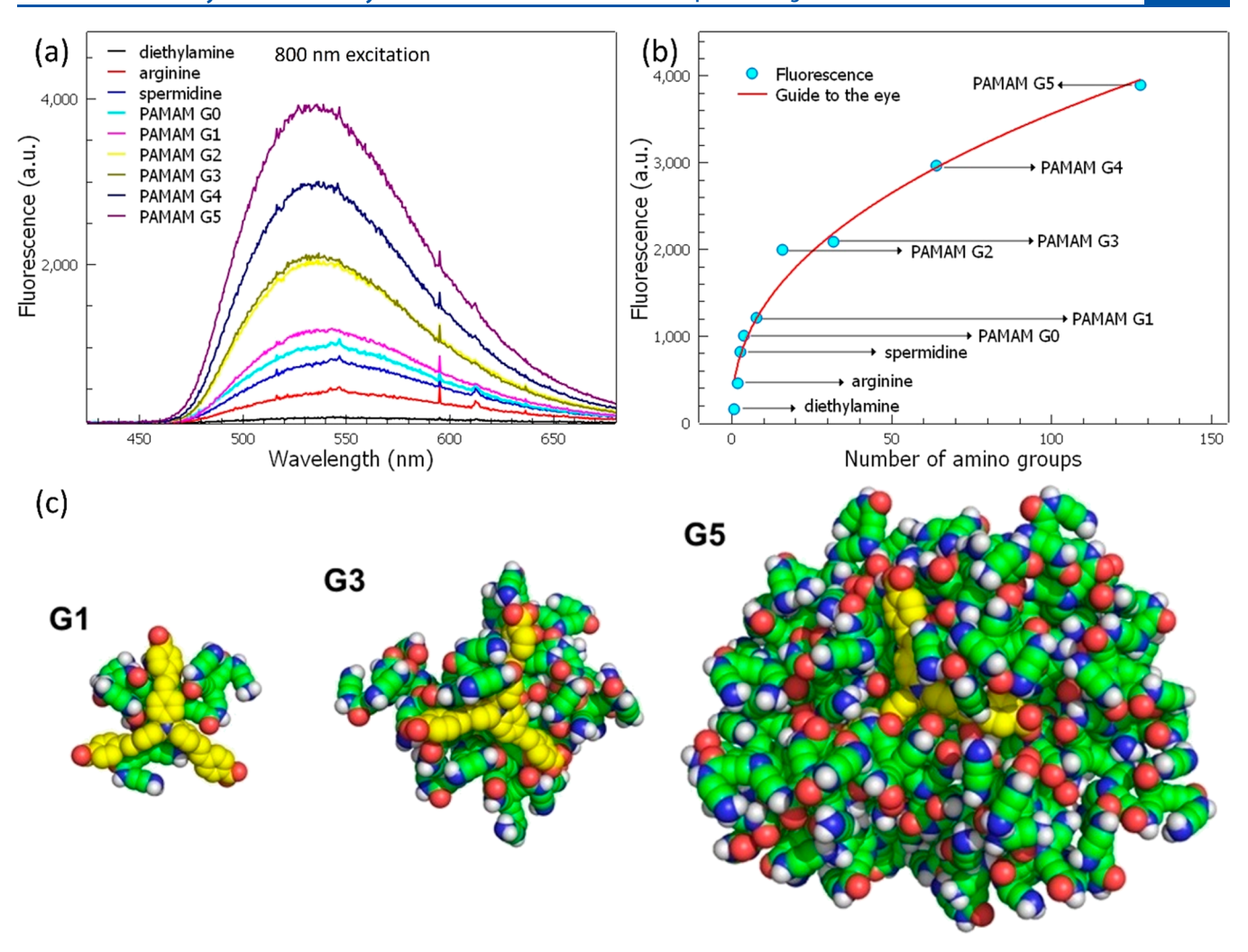


Figure 4. TP fluorescence spectra and docking simulation for compound 5 with dendrimers. (a) Measured TP fluorescence spectra. (b) Maximum fluorescence intensity plot as a function of amino group number in the dendrimers. We use the number of amino groups in dendrimers as an indicator of the complexity of the molecule. The red solid line is a guide to the eye. (c) Docking simulation of PAMAM G1, G3, and G5 dendrimers with dye compound 5. G1 represents the "generation 1" PAMAM dendrimer where the fluorescence of the compound is largely exposed to the solvent environment. G3 represents the "generation 3" PAMAM dendrimer where the majority of compound 5 interacts with the dendrimer. G5 represents the "Generation 5" PAMAM dendrimer, which largely encloses compound 5 and prevents the dye from the solvent environment. A total of nine binding states were performed, and their relative affinity is included in the Supporting Information. (Tables S1–S3).

results strongly suggest that the interactions between dendrimers (or protein molecules) and the dye molecules prevent the dye from interacting with water molecules. The dendrimers (or protein molecules) allow for the dye to be settled in its hydrophobic core where water interactions are minimal. Since the interaction between dye and water molecules may induce more non-radiative decay processes in TPA, the assembly of dye molecules and dendrimers (or protein molecules) can successfully recover the strength of TP fluorescence. This also explains the fluorescence enhancement trend (red solid line) in Figure 4b. As the dye molecules are better protected by more complex dendrimer molecules, the enhancement of fluorescence slows down. Once the interaction between the dye and water molecule are completely eliminated, the fluorescence stops to increase. However, it is hard to fully eliminate such interactions in the aqueous solution.

III.D. TP Fluorescence in Different Solvents and Centrifuge Experiments. To understand the interaction between dye and water molecules that is detrimental to the

fluorescence, we first hypothesize that hydrogen bonds between the solvent and the TPA molecule contribute to the TP fluorescence quenching since it is the most common interaction in aqueous solutions. As shown in Figure 5a, the fluorescence spectra of compound 5 in water (PBS), in methanol, and in DMSO are prepared and the TP fluorescence spectra for the three samples are presented. We have also tried acetone and THF solutions, but we did not show the data because the TPA molecules were not well soluble in these two solvents. Compared to the dye in the water solution, the fluorescence of dye molecules in methanol and DMSO solution was much stronger. The dye molecules in DMSO show the best fluorescence. The reason for choosing these three different solutions is based on their ability to form hydrogen bonding with our dye molecules. It is well known that organic molecules can easily form hydrogen bonds in the water solution (PBS), but it is harder to form hydrogen bonds in methanol and DMSO. Therefore, the results confirm that the more the hydrogen bonds form between dye and water molecules in the solution, the weaker the fluorescence. This

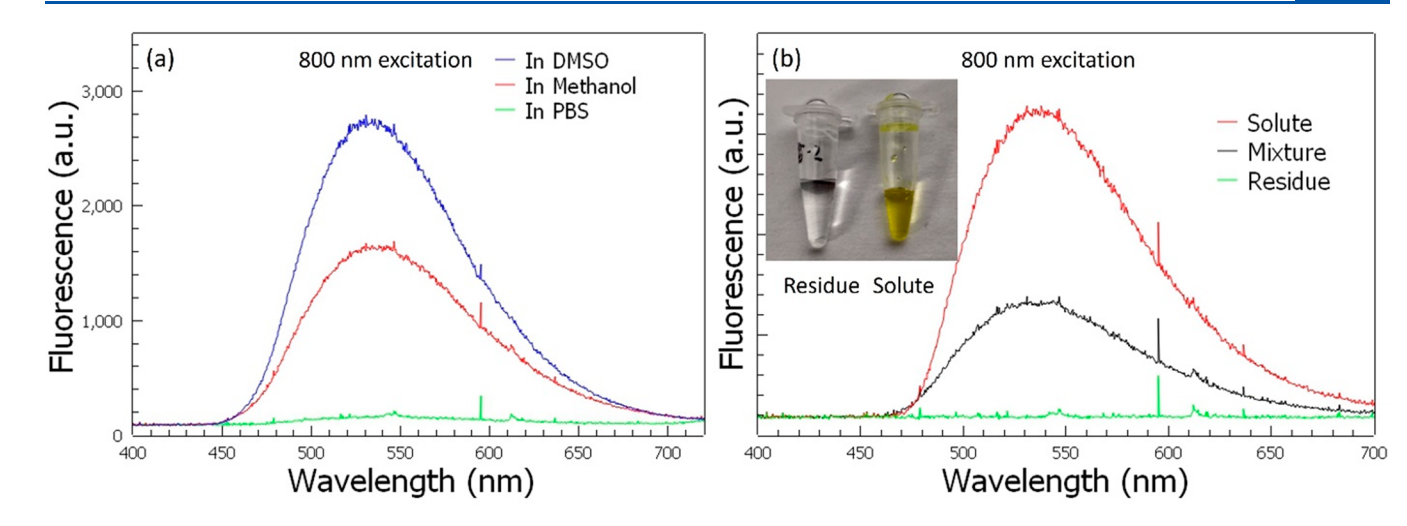


Figure 5. Solvent-dependent TP fluorescence and centrifuge experiments. (a) TP fluorescence spectra of dye compound 5 in PBS, methanol, and dimethyl sulfoxide (DMSO). (b) TP fluorescence spectra for samples in the centrifuge experiments. The inset shows the image of residue (compositions that pass through the centrifuge filter) and solute (compositions that cannot pass through the centrifuge experiments.

supports our hypothesis that the enhancement to the fluorescence of the TPA molecule and protein assembly in the water solution is due to the isolation of TPA molecules by protein from the water molecules. Now the question can be where is this hydrogen bonding formed? Based on our experimental and simulation results, the tri-anionic species at the end of the TPA molecule does not seem to contribute much to the fluorescence quenching or restoration since it docks with dendrimers with different sizes but the fluorescence enhancement only happens when the TPA molecule can be almost fully wrapped up. Therefore, it is more likely that the fluorescence emission intensity is greatly influenced by hydrogen bonding of the nitrogen core with water molecules. This localizes the lone pair electrons on nitrogen and limits the electron flow in the conjugation system, resulting in a decrease of florescence. This also explains the enhanced fluorescence upon adding protein molecules because the hydrophobic pocket of protein wraps the TPA molecules, preventing water molecules from accessing and forming a hydrogen bond with the nitrogen core. A more detailed mechanism of hydrogen bond influence on the electronic system in the TPA molecule can be revealed by further experiments and first-principle calculations, which will be carried out in our following work.

For the application purposes, we tested the strength of assembly between TPA molecules and protein in the water solution. We did the centrifuge experiment to compound 5 mixed with FBS. The centrifuge speed was 15,000 RPM, with a centrifuge time of 3 min. The centrifuge filter in our experiment only allows compositions with a molecular mass less than 10,000 g/mol to pass through. The protein usually has a large molecular mass, which cannot pass through the filter, while the dye molecule's molecular mass is less than 10,000 g/mol, which can easily pass through the filter if it is not strongly interacting with the protein. Based on the structures of proteins and the functional groups on the TPA molecules (negative charge on sulfate groups, polar amide groups, and hydrophobic phenyl vinylene groups on the arms), the interactions between protein and the dye could be a combination of an ion-ion or ion-dipole interaction, dipoledipole interaction, hydrogen bonding, and dispersion forces. In addition, our further simulation (Figure S4 in the Supporting

Information) shows that the vast majority of interactions are between the molecule's backbone and protein residues (either polar or non-polar). It is because of the overall effect of these interactions that the TPA molecules are firmly anchored inside protein molecules. Therefore, if the interaction between the TPA molecule and protein is strong enough, the TPA molecule should stay with protein without passing through the filter. Here, we define the "solute" as the composition that cannot pass through the filter and "residue" as the composition that passes through the filter after centrifuge experiments. As shown in Figure 5b, the TP fluorescence strength for solute is much stronger than that for residue and that for mixture before the centrifuge experiments. The results suggest that most of the dye molecules stay in the solute bonded with protein, contributing to the strong TP fluorescence. To further confirm this argument, we exhibited the image of residue and solute after centrifuge experiments in the inset of Figure 5b. The residue that passes through the filter is colorless and transparent, while the solute is yellow. According to the inset of Figure 1a, the dye molecule in the water solution without protein is also yellow. This proves that the majority of the dye molecules strongly bond with protein and they cannot pass through the centrifuge filter. Therefore, the assembly of the TPA dye and protein molecule is sturdy enough for future potential applications. To further boost the TP fluorescence and facilitate the application, strategies such as using plasmonics to enhance the nonlinear effects can be carried out, which can be very interesting and promising. 52,5

IV. CONCLUSIONS

In summary, the fluorescence quenching in the presence of water is an important effect that must be taken into account while designing water-soluble, environmentally friendly, and high fluorescence efficiency TPA molecules. We showed that the TP fluorescence of the present water-soluble triphenylamine-based all-organic compounds can be heavily boosted by the addition of protein molecules in water solution. Experimental and numerical simulation results support our hypothesis that blocking the formation of hydrogen bonds between the TPA and water molecules could be the cause of strong enhancement of TP fluorescence.

ASSOCIATED CONTENT

5 Supporting Information

The Supporting Information is available free of charge at https://pubs.acs.org/doi/10.1021/acs.jpcb.2c03514.

Comparison of the TPA fluorescence of compound 5 in pure water, in phosphate solution, in PBS solution, and in HCl solution; comparison of the TPA fluorescence of compound 5 in BSA and PBS solutions; ¹H and ¹³C NMR spectra of compounds 2–5; simulation of interactions between dye and BSA molecules by LigPLot+; relative affinities of different modes of binding between dye compounds 4 and 5 and G1, G3, G5, and BSA receptors; molecular docking parameters of search between dye compounds 4 and 5 and their respective ligands; and simulation details (PDF)

AUTHOR INFORMATION

Corresponding Authors

Yu Gong — Department of Physics and Astronomy, College of Charleston, Charleston, South Carolina 29424, United States; orcid.org/0000-0002-9357-9503; Email: gongy@cofc.edu

Xiangdong Bi — Department of Physical Sciences, Charleston Southern University, Charlest on, South Carolina 29485, United States; Email: Xbi@csuniv.edu

Nikki Chen – Department of Chemistry and Biochemistry, College of Charleston, Charleston, South Carolina 29424, United States; Email: chenn@g.cofc.edu

Marcello Forconi — Department of Chemistry and Biochemistry, College of Charleston, Charleston, South Carolina 29424, United States; orcid.org/0000-0002-5287-3757; Email: forconim@cofc.edu

Ming Hu − Department of Mechanical Engineering, University of South Carolina, Columbia, South Carolina 29208, United States; orcid.org/0000-0002-8209-0139; Email: HU@sc.edu

Authors

Narayanan Kuthirummal – Department of Physics and Astronomy, College of Charleston, Charleston, South Carolina 29424, United States

Alem Teklu – Department of Physics and Astronomy, College of Charleston, Charleston, South Carolina 29424, United States

Bo Gao – Department of Physics and Astronomy, Hunter College, City University of New York, New York, New York 10065, United States

Jacob Koenemann – Department of Physics and Astronomy, College of Charleston, Charleston, South Carolina 29424, United States

Nico Harris – Department of Physics and Astronomy, College of Charleston, Charleston, South Carolina 29424, United States

Christian Brennan – Department of Physics and Astronomy, College of Charleston, Charleston, South Carolina 29424, United States

Marisa Thomas – Department of Physical Sciences, Charleston Southern University, Charlest on, South Carolina 29485, United States; orcid.org/0000-0003-4813-7033

Taylor Barnes – Department of Physical Sciences, Charleston Southern University, Charlest on, South Carolina 29485, United States Complete contact information is available at: https://pubs.acs.org/10.1021/acs.jpcb.2c03514

Notes

The authors declare no competing financial interest.

ACKNOWLEDGMENTS

The authors would like to thank Professor Jay Forsythe from the Department of Chemistry and Biochemistry at the College of Charleston for his support of mass spectral measurements and guidance. Research reported in this publication was supported in part by the NSF and SC EPSCoR/IDeA Program under NSF Award #OIA-1655740 and GEAR CRP 20-GC02. The views, perspective, and content do not necessarily represent the official views of the SC EPSCoR Program nor those of the NSF.

REFERENCES

- (1) Sarih, N.; Myers, P.; Slater, A.; Slater, B.; Abdullah, Z.; AnuarTajuddin, H.; Maher, S. White Light Emission from a Simple Mixture of Fluorescent Organic Compounds. *Sci. Rep.* **2019**, *9*, 11834.
- (2) McCann, T.; Kosaka, N.; Koide, Y.; Mitsunaga, M.; Choyke, P.; Nagano, T.; Urano, Y.; Kobayashi, H. Activatable Optical Imaging with a Silica-Rhodamine Based near Infrared (Sir700) Fluorophore: A Comparison with Cyanine Based Dyes. *Bioconjugate Chem.* **2011**, 22, 2531–2538.
- (3) Kolemen, S.; Akkaya, E. Reaction-Based Bodipy Pobes for Selective Bio-Imaging. *Coord. Chem. Rev.* **2018**, 354, 121–134.
- (4) Sozmen, F.; Kolemen, S.; Kumada, H.; Ono, M.; Saji, H.; Akkaya, E. Designing Bodipy-Based Probes for Fluorescence Imaging of Beta-Amyloid Plaques. *RSC Adv.* **2014**, *4*, 51032–51037.
- (5) Galas, L.; Gallavardin, T.; Benard, M.; Lehner, A.; Schapman, D.; Lebon, A.; Komuro, H.; Lerouge, P.; Leleu, S.; Franck, X. "Probe, Sample, and Instrument (Psi)": The Hat-Trick for Fluorescence Live Cell Imaging. *Chemosensors* **2018**, *6*, 40.
- (6) Han, Y.; Li, M.; Qiu, F.; Zhang, M.; Zhang, Y. Cell-Permeable Organic Fluorescent Probes for Live-Cell Long-Term Super-Resolution Imaging Reveal Lysosome-Mitochondrion Interactions. *Nat. Commun.* **2017**, *8*, 1307.
- (7) Atilgan, S.; Ozdemir, T.; Akkaya, E. Selective Hg(Ii) Sensing with Improved Stokes Shift by Coupling the Internal Charge Transfer Process to Excitation Energy Transfer. *Org. Lett.* **2010**, *12*, 4792–4795.
- (8) Coskun, A.; Deniz, E.; Akkaya, E. A Sensitive Fluorescent Chemosensor for Anions Based on a Styryl-Boradiazaindacene Framework. *Tetrahedron Lett.* **2007**, *48*, 5359–5361.
- (9) Wu, D.; Sedgwick, A.; Gunnlaugsson, T.; Akkaya, E.; Yoon, J.; James, T. Fluorescent Chemosensors: The Past, Present and Future. *Chem. Soc. Rev.* **2017**, *46*, 7105–7123.
- (10) Bozdemir, O.; Guliyev, R.; Buyukcakir, O.; Selcuk, S.; Kolemen, S.; Gulseren, G.; Nalbantoglu, T.; Boyaci, H.; Akkaya, E. Selective Manipulation of Ict and Pet Processes in Styryl-Bodipy Derivatives: Applications in Molecular Logic and Fluorescence Sensing of Metal Ions. J. Am. Chem. Soc. 2010, 132, 8029—8036.
- (11) Liu, Y.; Su, Q.; Chen, M.; Dong, Y.; Shi, Y.; Feng, W.; Wu, Z.; Li, F. Near-Infrared Upconversion Chemodosimeter for in Vivo Detection of Cu2+ in Wilson Disease. *Adv. Mater.* **2016**, 28, 6625.
- (12) Mukherjee, S.; Thilagar, P. Organic White-Light Emitting Materials. *Dyes Pigm.* **2014**, *110*, 2–27.
- (13) Kim, H. M.; Cho, B. R. Small-Molecule Two-Photon Probes for Bioimaging Applications. *Chem. Rev.* **2015**, *115*, 5014–5055.
- (14) Park, Y. I.; Lee, K. T.; Suh, Y. D.; Hyeon, T. Upconverting Nanoparticles: A Versatile Platform for Wide-Field Two-Photon Microscopy and Multi-Modal in Vivo Imaging. *Chem. Soc. Rev.* **2015**, 44, 1302–1317.
- (15) Niu, W.; Guo, L.; Li, Y.; Shuang, S.; Dong, C.; Wong, M. S. Highly Selective Two-Photon Fluorescent Probe for Ratiometric

- Sensing and Imaging Cysteine in Mitochondria. *Anal. Chem.* **2016**, *88*, 1908–1914.
- (16) Li, J.; Cheng, F.; Huang, H.; Li, L.; Zhu, J. J. Nanomaterial-Based Activatable Imaging Probes: From Design to Biological Applications. *Chem. Soc. Rev.* **2015**, 44, 7855–7880.
- (17) Yuan, L.; Wang, L.; Agrawalla, B. K.; Park, S. J.; Zhu, H.; Sivaraman, B.; Peng, J.; Xu, Q. H.; Chang, Y. T. Development of Targetable Two-Photon Fluorescent Probes to Image Hypochlorous Acid in Mitochondria and Lysosome in Live Cell and Inflamed Mouse Model. J. Am. Chem. Soc. 2015, 137, 5930–5938.
- (18) LaFratta, C. N.; Fourkas, J. T.; Baldacchini, T.; Farrer, R. A. Multiphoton Fabrication. *Angew. Chem., Int. Ed.* **2007**, 46, 6238–6258.
- (19) Teran, N. B.; He, G. S.; Baev, A.; Shi, Y.; Swihart, M. T.; Prasad, P. N.; Marks, T. J.; Reynolds, J. R. Twisted Thiophene-Based Chromophores with Enhanced Intramolecular Charge Transfer for Cooperative Amplification of Third-Order Optical Nonlinearity. *J. Am. Chem. Soc.* **2016**, *138*, 6975–6984.
- (20) Yu, J.; Cui, Y.; Xu, H.; Yang, Y.; Wang, Z.; Chen, B.; Qian, G. Confinement of Pyridinium Hemicyanine Dye within an Anionic Metal-Organic Framework for Two-Photon-Pumped Lasing. *Nat. Commun.* **2013**, *4*, 2719.
- (21) Yu, J.; Cui, Y.; Wu, C. D.; Yang, Y.; Chen, B.; Qian, G. Two-Photon Responsive Metal-Organic Framework. *J. Am. Chem. Soc.* **2015**, 137, 4026–4029.
- (22) Huang, B. Native Point Defects in Cas: Focus on Intrinsic Defects and Rare Earth Ion Dopant Levels for up-Converted Persistent Luminescence. *Inorg. Chem.* **2015**, *54*, 11423–11440.
- (23) Lin, T. C.; Chung, S. J.; Kim, K. S.; Wang, X.; He, G. S.; Swiatkiewicz, J.; Prasad, P. N., Organics and Polymers with High Two-Photon Activities and Their Applications. In *Advances in Polymer Science*, Springer Nature: 2003; Vol. 161, pp. 157–193, DOI: 10.1007/3-540-45642-2 3.
- (24) Lu, K.; He, C.; Lin, W. A Chlorin-Based Nanoscale Metal-Organic Framework for Photodynamic Therapy of Colon Cancers. *J. Am. Chem. Soc.* **2015**, *137*, 7600–7603.
- (25) Zeng, C.; Shang, W.; Liang, X.; Chen, Q.; Chi, C.; Du, Y.; Fang, C.; Tian, J. Cancer Diagnosis and Imaging-Guided Photothermal Therapy Using a Dual-Modality Nanoparticle. *ACS Appl. Mater. Interfaces* **2016**, *8*, 29232–29241.
- (26) Chen, G.; Roy, I.; Yang, C.; Prasad, P. N. Nanochemistry and Nanomedicine for Nanoparticle-Based Diagnostics and Therapy. *Chem. Rev.* **2016**, *116*, 2826–2885.
- (27) Rad, Z.; Prewett, P.; Davies, G. High-Resolution Two-Photon Polymerization: The Most Versatile Technique for the Fabrication of Microneedle Arrays. *Microsyst. Nanoeng.* **2021**, *7*, 71.
- (28) Worthington, K.; Thompson, J.; Green, B.; Bunn, S.; Kaalberg, E.; Johnston, R.; Wiley, L.; Mullins, R.; Stone, E.; Guymon, C.; et al. Two-Photon Polymerization of High-Resolution 3d, Biodegradable Photoreceptor Cell Scaffolds. *Invest. Ophthalmol. Visual Sci.* 2017, 58, 3390.
- (29) Zheng, Y.; Sun, S.; Xu, L.; Ni, S.; Liu, W.; Huang, B.; Huang, Q.; Zhang, Q.; Lu, F.; Li, M. Arylamine-Coumarin Based Donor-Acceptor Dyads: Unveiling the Relationship between Two-Photon Absorption Cross-Section and Lifetime of Singlet Excited State Intramolecular Charge Separation. *Dyes Pigm.* **2019**, *165*, 301–307.
- (30) Xu, L.; Zhang, J.; Yin, L.; Long, X.; Zhang, W.; Zhang, Q. Recent Progress in Efficient Organic Two-Photon Dyes for Fluorescence Imaging and Photodynamic Therapy. *J. Mater. Chem.* C 2020, 8, 6342–6349.
- (31) Liang, X.; Zhang, Q. Recent Progress on Intramolecular Charge-Transfer Compounds as Photoelectric Active Materials. *Sci. China Mater.* **2017**, *60*, 1093.
- (32) Xu, L.; Lin, W.; Huang, B.; Zhang, J.; Long, X.; Wenying, Z.; Qichun, Z. The Design Strategies and Applications for Organic Multi-Branched Two-Photon Absorption Chromophores with Novel Cores and Branches: A Recent Review. *J. Mater. Chem. C* **2021**, *9*, 1520–1536.

- (33) Xu, L.; Zhu, H.; Long, G.; Zhao, J.; Li, D.; Ganguly, R.; Li, Y.; Xu, Q.; Zhang, Q. 4-Diphenylamino-Phenyl Substituted Pyrazine: Nonlinear Optical Switching by Protonation. *J. Mater. Chem. C* **2015**, 3, 9191–9196.
- (34) Collini, E. Cooperative Effects to Enhance Two-Photon Absorption Efficiency: Intra- Versus Inter-Molecular Approach. *Phys. Chem. Phys.* **2012**, *14*, 3725–3736.
- (35) Ye, C.; Zhou, L.; Wang, X.; Liang, Z. Photon Upconversion: From Two-Photon Absorption (Tpa) to Triplet-Triplet Annihilation (Tta). *Phys. Chem. Chem. Phys.* **2016**, *18*, 10818–10835.
- (36) Brousmiche, D. W.; Serin, J. M.; Fréchet, J. M. J.; He, G. S.; Lin, T.-C.; Chung, S.-J.; Prasad, P. N.; Kannan, R.; Tan, L.-S. Fluorescence Resonance Energy Transfer in Novel Multiphoton Absorbing Dendritic Structures. *J. Phys. Chem. B* **2004**, *25*, 8592–8600
- (37) Wan, Y.; Yan, L.; Zhao, Z.; Ma, X.; Guo, Q.; Jia, M.; Lu, P.; Ramos-Ortiz, G.; Maldonado, J. L.; Rodríguez, M.; et al. Gigantic Two-Photon Absorption Cross Sections and Strong Two-Photon Excited Fluorescence in Pyrene Core Dendrimers with Fluorene/Carbazole as Dendrons and Acetylene as Linkages. *J. Phys. Chem. B* **2010**, *114*, 11737–11745.
- (38) Gautam, P.; Wang, Y.; Zhang, G.; Sun, H.; Chan, J. M. W. Using the Negative Hyperconjugation Effect of Pentafluorosulfanyl Acceptors to Enhance Two-Photon Absorption in Push—Pull Chromophores. *Chem. Mater.* **2018**, *30*, 7055—7066.
- (39) Kim, H. M.; Lee, Y. O.; Lim, C. S.; Kim, J. S.; Cho, B. R. Two-Photon Absorption Properties of Alkynyl-Conjugated Pyrene Derivatives. *J. Org. Chem.* **2008**, *73*, 5127–5130.
- (40) Jiang, Y.; Wang, Y.; Hua, J.; Tang, J.; Li, B.; Qian, S.; Tian, H. Multibranched Triarylamine End-Capped Triazines with Aggregation-Induced Emission and Large Two-Photon Absorption Cross-Sections. *Chem. Commun.* **2010**, *46*, 4689–4691.
- (41) Wang, X.; Jin, F.; Chen, Z.; Liu, S.; Wang, X.; Duan, X.; Tao, X.; Jiang, M. A New Family of Dendrimers with Naphthaline Core and Triphenylamine Branching as a Two-Photon Polymerization Initiator. *J. Phys. Chem. C* **2011**, *115*, 776–784.
- (42) Zhang, X.; Hassine, S. B.; Richy, N.; Mongin, O.; Blanchard-Desce, M.; Paul, F.; Paul-Roth, C. O. New Porphyrin Dendrimers with Fluorenyl-Based Connectors: A Simple Way to Improving the Optical Properties over Dendrimers Featuring 1,3,5-Phenylene Connectors. New J. Chem. 2020, 44, 4144–4157.
- (43) Xu, L.; Long, X.; Kang, F.; Deng, Z.; He, J.; Yang, S.; Wu, J.; Yin, L.; Jiang, X.-F.; Lu, F.; et al. Simultaneously Enhancing Aggregation-Induced Emission and Boosting Two-Photon Absorption of Perylene Diimides through Regioisomerization. *J. Mater. Chem. C* **2022**, *10*, 7039–7048.
- (44) Long, X.; Wu, J.; Yang, S.; Deng, Z.; Zheng, Y.; Zhang, W.; Jiang, X.-F.; Lu, F.; Li, M.-D.; Xu, L. Discovery of and Insights into One-Photon and Two-Photon Excited Acq-to-Aie Conversion Via Positional Isomerization. *J. Mater. Chem. C* **2021**, *9*, 11679–11689.
- (45) Liu, Z.; Lu, T. Optical Properties of Novel Conjugated Nanohoops: Revealing the Effects of Topology and Size. *J. Phys. Chem. C* **2020**, *124*, 7353–7360.
- (46) Gong, Y.; Hou, G. L.; Bi, X.; Kuthirummal, N.; Teklu, A. A.; Koenemann, J.; Harris, N.; Wei, P.; Devera, K.; Hu, M. Enhanced Two-Photon Absorption in Two Triphenylamine-Based All-Organic Compounds. *J. Phys. Chem. A* **2021**, *125*, 1870–1879.
- (47) Hanwell, M.; Curtis, D.; Lonie, D.; Vandermeersch, T.; Zurek, E.; Hutchison, G. Avogadro: An Advanced Semantic Chemical Editor, Visualization, and Analysis Platform. *Aust. J. Chem.* **2012**, *4*, 17.
- (48) Morris, G.; Huey, R.; Lindstrom, W.; Sanner, M.; Belew, R.; Goodsell, D.; Olson, A. Autodock4 and Autodocktools4: Automated Docking with Selective Receptor Flexibility. *J. Comput. Chem.* **2009**, 30, 2785–2791.
- (49) Trott, O.; Olson, A. Software News and Update Autodock Vina: Improving the Speed and Accuracy of Docking with a New Scoring Function, Efficient Optimization, and Multithreading. *J. Comput. Chem.* **2010**, *31*, 455–461.

- (50) Matsarskaia, O.; Buhl, L.; Beck, C.; Grimaldo, M.; Schweins, R.; Zhang, F.; Seydel, T.; Schreiber, F.; Roosen-Runge, F. Evolution of the Structure and Dynamics of Bovine Serum Albumin Induced by Thermal Denaturation. *Phys. Chem. Chem. Phys.* **2020**, 22, 18507—18517.
- (51) Lee, J.; Robinson, G. Electron Hydration Dynamics Using the 2-Anilinonaphthalene Precursor. *J. Am. Chem. Soc.* **1985**, *107*, 6153–6156.
- (52) Chen, Y.; Cheng, Y.; Sun, M. Nonlinear Plexcitons: Excitons Coupled with Plasmons in Two-Photon Absorption. *Nanoscale* **2022**, 14, 7269–7279.
- (53) Cui, L.; Li, R.; Mu, T.; Wang, J.; Zhang, W.; Sun, M. In Situ Plasmon-Enhanced Cars and Tpef for Gram Staining Identification of Non-Fluorescent Bacteria. *Spectrochim. Acta A Mol. Biomol. Spectrosc.* **2022**, *264*, No. 120283.